# Annular Truncated Plug Nozzle Flowfield and Base Pressure Characteristics

WAYNE P. SULE* AND THOMAS J. MUELLER†
*University of Notre Dame, Notre Dame, Ind.*

**The flowfield and base pressure characteristics of an internal-external-expansion, truncated plug nozzle are described over the pressure ratio range from "open" wake to "closed" wake conditions. The effect of plug length on these characteristics, including the process of wake "closure" is also presented. An existing method for calculating the flowfield and base pressure, for closed wake operation, is modified to include the internal shock wave generated near the shroud exit. The supersonic portion of the flow is calculated using rotational axisymmetric method of characteristics. The technique of Hartree is employed so that the downstream characteristic point locations can be chosen to fit the developing flowfield. An overexpansion technique is used to detect the internal shock wave in the vicinity of the shroud exit so that its effect on the plug base pressure could be determined. Good agreement between the analytical results and experimental data is obtained for closed wake operations.**

## Nomenclature

| | |
|---|---|
| $A$ | = area |
| $L$ | = plug or shroud length from throat |
| $M$ | = Mach number |
| $P$ | = pressure |
| $R, r$ | = radius |
| $T$ | = temperature |
| $u$ | = velocity in $x$ direction |
| $X, Y$ | = coordinates of the reference (inviscid) coordinate system |
| $\bar{X}$ | = axial coordinate with origin at shroud exit |
| $x, y$ | = coordinates of the intrinsic (viscous) coordinate system |
| $\alpha$ | = plug angle |
| $\gamma$ | = ratio of specific heats |
| $\eta$ | = dimensionless coordinate ($= \sigma y/x$) |
| $\theta$ | = streamline angle |
| $\mu$ | = Mach angle |
| $\nu$ | = Prandtl-Meyer turn angle |
| $\sigma$ | = jet spread parameter |
| $\phi$ | = velocity ratio ($= u/u_a$) |

*Subscripts*

| | |
|---|---|
| 1, 2, 3, 4 | = stations for the basic flow model |
| $a$ | = conditions in the external stream adjacent to the mixing region |
| at | = atmospheric conditions |
| $b$ | = conditions at the base of the plug |
| $d$ | = streamline whose kinetic energy is just sufficient to enter the recompression region |
| $j$ | = condition along the jet boundary separating streamline |
| $m$ | = coordinate shift in the mixing theory due to the momentum integral |
| max | = refers to a maximum value |
| $ne$, $nt$, 01 | = nozzle exit, throat and stagnation conditions, respectively |
| $R$ | = condition along the $R$-streamline |
| sh | = shroud |
| $w$ | = wake |

Presented as Paper 73-137 at the AIAA 11th Aerospace Sciences Meeting, Washington, D.C., January 10-12, 1973; submitted February 5, 1973; revision received June 4, 1973. Research supported by NASA under Contract NAS 8-25601 and the Department of Aerospace and Mechanical Engineering, and was part of the Ph.D. dissertation of W. P. Sule. The authors gratefully acknowledge the efforts of H. Ackert for preparing the figures and T.V. Giel for allowing us to use some of his experimental data for ATP2 and for his helpful comments during the preparation of this manuscript.

Index categories: Airbreathing Propulsion, Subsonic and Supersonic; Electric and Advanced Space Propulsion; Jets, Wakes, and Viscid-Inviscid Flow Interactions.

*Research Assistant; presently at the Naval Air Engineering Center, Philadelphia Naval Base, Philadelphia, Pa. Member AIAA.

†Professor. Associate Fellow AIAA.

## Introduction

THE performance of advanced air-breathing and rocket propulsion systems may be improved by using altitude compensating nozzles. These exhaust nozzles will be required to operate efficiently from sea level to extremely high altitudes. The presence of a viscous separated wake and free expansion surfaces within the nozzle flowfield, as shown in Fig. 1, enables

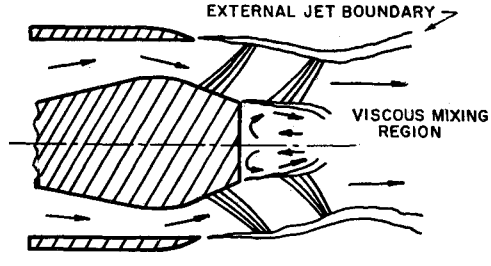


a. LOW ALTITUDE OPERATION, "OPEN WAKE"

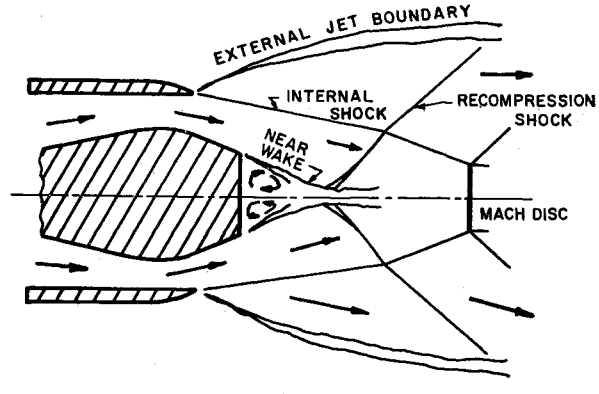


b. HIGH ALTITUDE OPERATION, "CLOSED WAKE"

**Fig. 1 Essential features of internal-external-expansion axisymmetric truncated plug nozzle flowfields.**

a truncated plug nozzle to adjust to ambient conditions, and thereby reduce overexpansion losses at low altitudes and minimize underexpansion losses at high altitudes. Truncated plug exhaust nozzles may be integrated into any air-breathing or rocket engine and have the added advantage of reduced size and weight.

At low values of chamber to ambient pressure ratio (Fig. 1a) the separated flow region is "open" (i.e., sensitive to ambient conditions) and unsteady in nature. Due to the relatively high ambient pressure, the external boundary is inclined toward the nozzle axis. The combined effects of the "open wake" and the position of the external boundary result in a low over-all nozzle area ratio during low altitude operation. As the chamber to ambient pressure ratio increases, the jet mixing region (shear layer between nozzle exhaust flow and separated flow region) moves toward the nozzle axis and the external boundary moves away from the nozzle axis. This produces a continously increasing effective nozzle area ratio as the vehicle altitude increases. During the open wake regime of operation the base pressure is essentially equal to the ambient pressure. At some point in the trajectory, when the chamber to ambient pressure ratio has increased sufficiently, the wake "closes" (Fig. 1b) and the separated base region is no longer sensitive to ambient conditions. The structure of the nozzle flowfield (including the base pressure) for closed wake operation is of particular interest since this represents design operating conditions. Also, for most nozzles of practical interest, the wake would be closed for the major portion of the flight. Nozzle area ratio adjustment still occurs during closed wake operation, since the external boundary continues to move away from the nozzle axis as the ambient pressure decreases. This continual adjustment of area ratio with altitude is the reason for the designation altitude compensating nozzle.

## Experimental Studies

A series of experiments were performed on various plug nozzles in the Notre Dame Nozzle Thrust Facility (NTF). These experiments also produced the experimental data used to verify the theoretical results.

Two axisymmetric internal-external-expansion plug nozzles were designed for Mach numbers of 1.90 (ATP1) and 2.00 (ATP2) based on the over-all area ratio, $A_{ne}/A_{nt}$. The plugs were conical in shape and converged toward the axis at an angle of 10°. The plug lengths, etc., are included in Tables 1 and 2. All the plugs were instrumented with static pressure taps in the base. Other static pressure taps were located on the plug surface for all ATP2 plugs and along the ATP1 shroud surface. The plugs were mounted to a webbed centerbody, which was contained in a buffer section. Tubing from the pressure taps in the plugs exited from the NTF through this buffer section. The shroud contours were cylindrical and extended a distance of 0.300 in. from the throat. The throat areas were 0.330 in.$^2$ and 0.602 in.$^2$ for ATP1 and ATP2, respectively. A more complete description of the experimental equipment and procedure may be found in Ref. 1.

**Table 1 Axisymmetric truncated plug nozzle model ATP1[a]**

| Length ratio, $L/L_{max}$ | Length from throat $L$, in. | Base radius, $r_b$, in. |
|---|---|---|
| 0.2184 | 0.300 | 0.188 |
| 0.2766 | 0.380 | 0.174 |
| 0.3275 | 0.450 | 0.162 |
| 0.3785 | 0.520 | 0.150 |
| 0.4290 | 0.590 | 0.137 |
| 0.4802 | 0.660 | 0.125 |

[a]Throat area, $A_{nt} = 0.330$ in.$^2$; shroud radius, $r_{sh} = 0.405$ in.; shroud length from throat, $L_{sh} = 0.300$ in.; and maximum plug length, $L_{max} = 1.374$ in.

**Table 2 Axisymmetric truncated plug nozzle model ATP2[a]**

| Length ratio, $L/L_{max}$ | Length from throat, $L$, in. | Base radius, $r_b$, in. |
|---|---|---|
| 0.1449 | 0.300 | 0.312 |
| 0.2327 | 0.482 | 0.280 |
| 0.2766 | 0.573 | 0.260 |
| 0.3275 | 0.678 | 0.245 |
| 0.3785 | 0.783 | 0.227 |

[a]Throat area, $A_{nt} = 0.602$ in.$^2$; shroud radius, $r_{sh} = 0.568$ in.; shroud length from throat, $L_{sh} = 0.300$ in.; and maximum plug length, $L_{max} = 2.070$ in.

### Base Pressure Characteristics

The base pressure characteristics for the six nozzle configurations of ATP1 are shown in Fig. 2. These data indicate that during a large portion of the open wake operation, the base pressure is essentially equal to the ambient pressure for all the plug length ratios used. At a particular value of the over-all pressure ratio (depending upon nozzle geometry) the wake closes. Once closed wake operation has been reached, the base pressure remains constant with further decreases in $P_{at}/P_{01}$.

For the two longer plug lengths ($L/L_{max} = 0.4290$ and 0.4802) there is a deviation from the normal open wake operation. This appears as an apparent discontinuity in the base pressure ratio between the values of 0.20 and 0.40 in the over-all pressure ratio. As $P_{at}/P_{01}$ decreases toward the "jump" the base pressure decreases below ambient, as shown by the steepening slope of the data in this region. After the jump the same trend continues until the wake closes. A possible explanation for this behavior was obtained from a series of shadowgraphs showing the development of the flowfield, Fig. 3. The letters identifying the photographs in Fig. 3 correspond to the labeled points in Fig. 2. The jump in the data occurs between Figs. 3b and 3c. In Fig. 3b the oblique shock which is reflected from the plug surface intersects the free shear layer originating from the shroud tip and is reflected as an expansion which intersects the plug surface a short distance upstream of the base. In Fig. 3c this reflected expansion does not intersect the plug but instead intersects the free shear layer downstream of the plug base. Apparently this expansion shown in Fig. 3b accelerates the flow upstream of the base which results in a reduced base pressure as indicated in Fig. 2. Once the reflected expansion has moved downstream of the plug base, in Fig. 3c, the Mach number approaching the base would be lower resulting in a higher base pressure and thus producing the jump shown in Fig. 2.

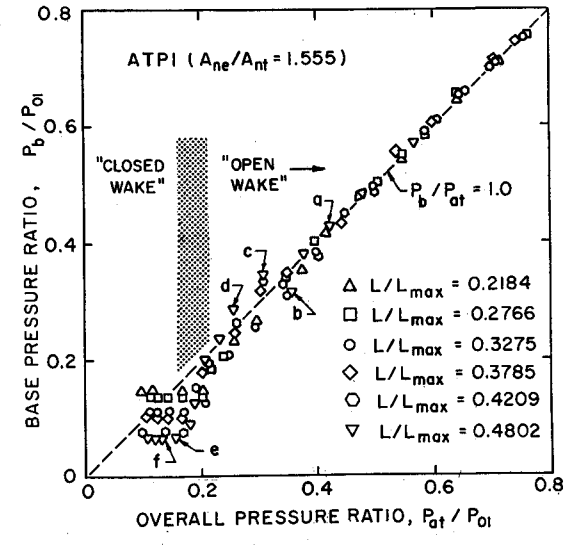


**Fig. 2 Base pressure characteristics of an axisymmetric truncated plug nozzle.**

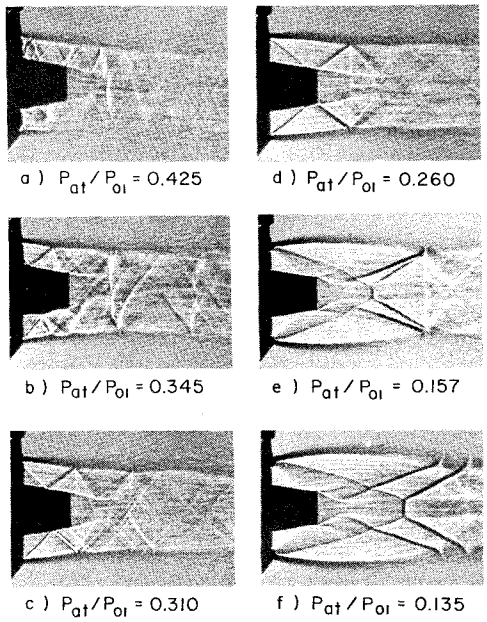


**Fig. 3 Shadowgraph sequence showing axisymmetric truncated plug nozzle flowfield develpment for ATP1 and $L/L_{max} = 0.4802$.**

Verification for this explanation is provided by noting the value of over-all pressure ratio at which the jump in the data occurs. If the discontinuity in base pressure is caused by the reflected expansion moving off the plug, the phenomenon would be expected to occur at a lower value of $P_{at}/P_{01}$ as the plug length is increased. This is because the point of impingement of the expansion moves down the plug as the over-all pressure ratio is decreased. For a longer plug, the expansion would reach the plug corner at a lower value of $P_{at}/P_{01}$ than for a shorter plug. This trend is indeed observed in the base pressure data.

The variation of the closed wake base pressure with plug length ratio is presented in Fig. 4. The base pressure ratio decreases with increasing plug length ratio. The theoretical curves on Fig. 4 will be discussed in a later section. Another very important trend to be found in the base pressure characteristics data is the variation in over-all pressure ratio at which the wake closes as a function of plug length. This effect is plotted explicitly in Fig. 5. The value of $P_{at}/P_{01}$ at wake closure decreases with increasing plug length and area ratio. This means that, in general, closed wake operation would be reached at lower altitudes for shorter plugs. This result points to one of the reasons for using shorter plugs. The calculation of performance for a given mission is greatly facilitated if the base pressure is constant (closed wake condition) for the longest period possible. In addition, open wake operation could possibly lead to flow oscillations which might produce prohibitive vibrations.

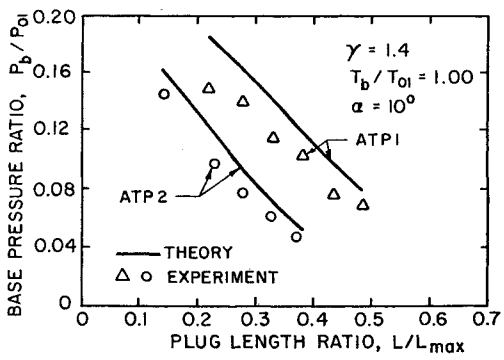


**Fig. 4 Experimental and analytical variations of base pressure ratio with plug length ratio.**

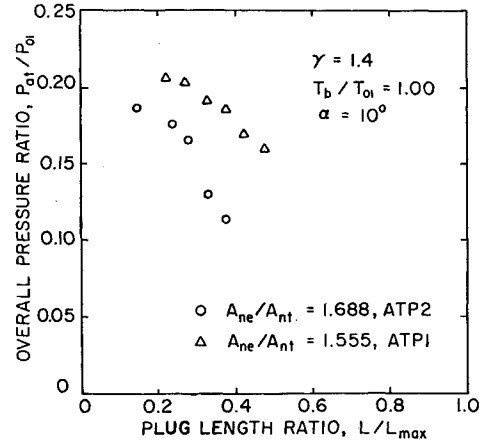


**Fig. 5 Effect of plug length ratio on over-all pressure ratio at "wake closure."**

### External Flowfield Characteristics

The external flowfield for the nozzle ATP1 was investigated in detail. For each of the nozzle configurations, shadowgraphs of the flowfield were obtained for at least ten different over-all pressure ratios. The values of $P_{at}/P_{01}$ were selected so that the nozzles would be operating in the closed wake regime. Certain basic closed wake flow characteristics were found to be common to all nozzle configurations (e.g., see Fig. 3f). These include the external jet boundary emanating from the shroud exit, the expansion from the shroud exit, the strong internal shock originating in the vicinity of the shroud exit, the lip shock originating in the vicinity of the plug corner, and the recompression shock wave.

The movement of the internal shock with changes in the over-all pressure ratio was very distinct in the photographs. In the shadowgraph sequence for each plug length the angle of the internal shock wave from the horizontal increased noticeably as the value of $P_{at}/P_{01}$ increased. This happened as the shock penetrated into the expansion fans from both the plug corner and the shroud exit (i.e., into higher Mach number regions).

Although the lip shock and the internal shock are consequences of the same phenomena, their different locations dictate different influences on the flowfield and in particular on the base pressure. The internal shock causes the base pressure to decrease by preventing compression waves from the constant pressure boundary from influencing the near wake. In contrast the lip shock occurs with separation of the viscous near wake shear layer distorting the velocity profile of the viscous mixing layer thus resulting in an unknown influence on the near wake. Furthermore the lip shock will cause an increase in the pressure in the inviscid flow along the near wake. This second influence, however, is expected to diminish in the downstream direction as the lip shock strength diminishes.

In all the shadowgraphs which have been made of the truncated plug nozzle flowfields, the lip shock is at most barely visible indicating that it is weak. The lip shock has been extensively studied by Hama.[2] His results indicate that when the plug surface is boattailed the lip shock strength is greatly reduced. In addition, when the boundary layer approaching separation is turbulent, the lip shock almost totally disappears and will not appreciably affect the flow.

## Analytical Studies

In order to optimize design, predict performance, and design altitude test facilities for this type of nozzle, it is desirable to calculate the entire nozzle flowfield. The method of solution presented is for closed wake operation. This analytical treatment of the nozzle flowfield must incorporate the

important characteristics shown in Fig. 1b. The pressure acting on the plug base is very important, since it can contribute significantly to the total thrust or drag of the nozzle. The strong internal shock wave emanating from the shroud exit must also be included in the over-all solution. This shock penetrates deeply into the flowfield, and may interact with the near wake region. The presence of this shock will certainly have an effect on the location of the external jet boundary, and will have an effect on the plug base pressure. The location of the external boundary is important when testing nozzles in altitude test facilities, or if it impinges on adjacent parts of the vehicle surface.

The object of the present analytical study was to modify and extend the analytical solution of Hall and Mueller[3] to include the internal shock wave. The supersonic inviscid portion of the flow was calculated using the rotational method of characteristics. The separated flow region was determined by an integral method, and coupled to the method of characteristics by an iterative technique. Solutions were obtained for a variety of T–P nozzle geometries and over-all pressure ratios.

### Flow Model

Figures 1b and 6a show the essential features of the flowfield under consideration. The nozzle geometry is a typical internal-external-expansion truncated plug nozzle with nonisentropic contours. Once the flow has passed through the sonic line and begins to accelerate supersonically, the governing equation for the inviscid flow becomes hyperbolic and can be solved by the method of characteristics. This method has been shown to be very accurate for a variety of supersonic flows of the type under investigation.[3,4] The axisymmetric rotational method of characteristics is used in the present study, in order to include the entropy gradients downstream of the internal shock in the calculations. Entropy gradients from other sources are not allowed.

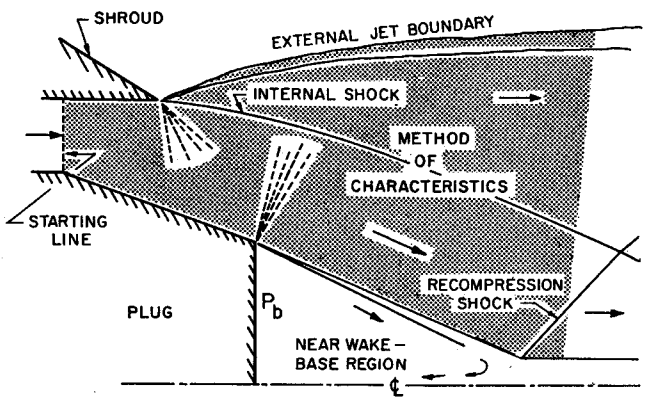


a) Inviscid flowfield.

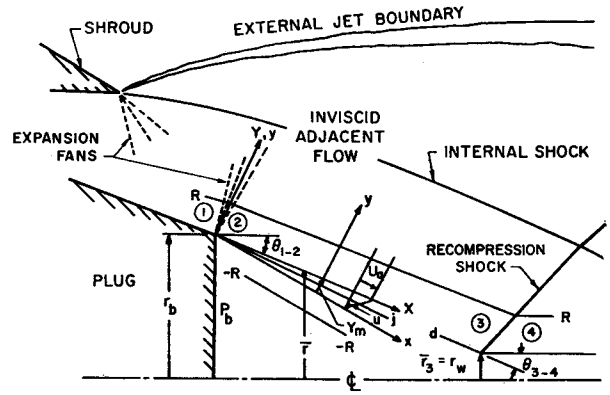


b) Turbulent base pressure flow model.

**Fig. 6 Flow model used to determine the base pressure and inviscid plug nozzle flowfield.**

The entire flowfield between the nozzle surfaces and between the external jet boundary and separated base region is assumed to be inviscid and adiabatic. In addition, the boundary layers on the nozzle surfaces are assumed to be negligible. For all cases studied, the nozzle is assumed to be exhausting into still air.

The solution of the separated base region is obtained using an extension of the flow model developed by Zumwalt,[5] and later modified by Mueller[6,7] and Hall and Mueller[3] and is shown in Fig. 6b. With this analysis a conical wake is assumed whereby the pressure field impressed on the separated shear layer is determined by the method of characteristics over a conetail. This method establishes the general features of the entire base region, while calculating the base pressure.

The conetail surface provides the boundary for the method of characteristics in the base region. However, the solution of the base region (including the orientation of the conetail) requires inputs from the method of characteristics. Therefore, in addition to the iterative base pressure solution, the solution of the entire nozzle flowfield becomes iterative.

The standard method of characteristics was used to construct the solution of the nozzle flowfield from the starting line to the shroud exit. In order to compare the present results with those of Hall and Mueller[3] a vertical starting line was used. A special routine was developed such that a row of characteristic points could be established at the nozzle exit plane. This step was necessary in order to control the depth of penetration of the expansion at the shroud exit corner.

A modified calculation method was used for the method of characteristics downstream of the shroud exit. This procedure was introduced by Hartree[8] and therefore will be referred to as the Hartree Technique. This scheme is most useful in the vicintiy of an imbedded shock wave. Calculations across a shock wave require a characteristic point on both sides of the shock. In the standard method, these shock points must be determined by interpolation between neighboring points. This necessitates storing the location of surrounding points with respect to the shock location. With the Hartree Technique, shock wave points are handled with no more difficulty than a regular interior point.

### Corner expansion

A special calculation procedure was required to properly model the corner expansion. The solution is known at the shroud exit plane from the upstream calculations. Using the point at the exit corner and the next point below it on the exit plane, a standard method of characteristics calculation is performed, and a linear interpolation is used to determine the flow conditions on a "solution" line. This defines the first point in the expansion fan. The points below this first point are calculated using the Hartree Technique. Succeeding points in the expansion fan are calculated by assuming a Prandtl-Meyer expansion at the exit corner. The total change in flow variables through the expansion corner is then divided into a number of equal steps (the number depending on the accuracy desired). The flow variables at the corner are set equal to the values for the next step in the expansion, and this point is used in conjunction with the previous point on the solution line in a standard calculation. Linear interpolation is again used to place each new point on the solution line. This process is continued until the expansion fan has been calculated.

In order to determine the intersection of the constant pressure boundary with the new solution line, a line is extended through the exit corner at an angle equal to the flow angle after the expansion. Conditions along this line and at the first boundary point are set equal to the flow properties after the expansion. Characteristic points are then placed on the

constant pressure boundary at equal increments. The solution between the last point in the expansion fan and the constant pressure boundary point is constructed in the same manner as described above for expansion fan points.

#### Shock wave detection and development

In the method of characteristics solution, a shock wave is detected when two characteristics of the same family intersect. The constant pressure jet boundary originating at the exit is curved, and the characteristics emanating from this boundary will eventually intersect. The standard procedure is to expand the flow to the ambient pressure, and then continue the calculations downstream until a shock is detected., With this method the initial shock wave point is not identified until a considerable distance downstream. In the actual case the shock originates near the shroud corner. The inviscid flow fails to negotiate the corner and overexpands to a pressure below the ambient pressure. The boundary layer overexpands with the inviscid flow, and the internal shock forms to return the pressure on the boundary back to the actual ambient pressure.

Because of the importance of detecting the internal shock wave in the vicinity of the corner where it is initiated, a modified calculation scheme was developed for this region. In order to partially account for the overexpansion, the flow is initially expanded to a pressure below the ambient pressure. After several steps downstream, the boundary pressure is returned to its actual value and the calculations proceed normally. Using this method, the initial shock wave point is detected close to the nozzle exit, and therefore the exhaust flow is more accurately modeled. It should be pointed out that overexpanding the flow at the corner is totally consistent with the situation in the actual case. Boynton[9] has shown that the presence of the boundary layer produces a flow angle after the expansion, which is well above that predicted by inviscid theory.

Since the Hartree Technique does not follow characteristics, it was modified for this purpose. New points, at which solutions are to be obtained, are established by the intersection of characteristics from the external boundary with the new solution line. As the iteration proceeds, the value of the axial coordinate is held constant while the value of the radial coordinate is allowed to "float." In this manner, the solution proceeds along characteristics. When two characteristics intersect, the initial shock wave angle is set equal to the average angle of the intersecting characteristics. This shock angle is projected downstream to the next solution line. From this point on, characteristics are no longer followed.

#### Lip shock

A similar overexpansion at the plug corner produces the lip shock wave which has been studied in the experimental phase of this research. Results show that the lip shock strength is greatly reduced in the cases studied, therefore the lip shock was not included in the theoretical calculations. The flow is expanded to the assumed base pressure and the solution is continued along a conetail until the predetermined wake radius is reached. At this stage, the base pressure solution is initiated.

#### Basic pressure solution

The flow model used for the determination of the turbulent base pressure is shown in Fig. 6b. A complete derivation of the governing equations is presented in Ref. 10. This model was developed by Zumwalt[5, 11] and later modified by Mueller[6, 7] and Hall and Mueller.[3] In addition to using the restricted mixing theory of Korst,[12] the following conditions are imposed on the base flow model: a) The boundary layer approaching the separation corner is neglected, although fully turbulent mixing is assumed. b) An insentropic expansion takes place at the base corner from 1 to 2, and the effect of a lip shock is ignored. c) The inviscid flow past a conetail, using the rotational method of characteristics, is utilized to define the pressure field impressed on the mixing region from 2 to 3. This conetail surface also serves as the "corresponding inviscid jet boundary." d) The pressure normal to the "corresponding inviscid jet boundary" is assumed to be constant within and near the mixing region at each cross section. e) Velocity profile similarity is assumed in the mixing region. The error function velocity distribution is located within the intrinsic coordinates $x$, $y$, and is represented by $X \simeq x$ and $Y = y - y_m(x)$ where $y_m(0) = 0$. This coordinate shift is a consequence of using the restricted mixing theory of Korst. f) Recompression is assumed to result from an oblique shock turn from 3 to 4 at an empirically determined trailing wake radius ratio.

The control volume between cross sections 2 and 3 is bounded by streamlines $R$ and $-R$ which were defined by Zumwalt[5] such that the cross-sectional area normal to the direction of the flow would remain nearly constant, and the $P \cdot dA$ pressure force could be neglected in the momentum equation. The momentum equation in the axial direction was formulated using geometrical relations and the relationship between the viscous and inviscid coordinate systems. This equation was solved simultaneously with the combined viscous and inviscid continuity equations written for the control volume between cross sections 2 and 3. For the error function velocity profile, $\phi = \frac{1}{2}(1 + \text{erf}\,\eta)$, where $\phi + u/u_a$ and $\eta = \sigma y/x$, it was found that $\eta_R = 3$ was large enough for $\phi_j$ to approach its asymptotic value. The result of this analysis is a nonlinear equation which allows one to locate the $j$-streamline at cross section 3. (Reference 5 and 10 give details of the analysis.) In order to determine $\eta_{j3}$ and therefore $\phi_{j3}$ for a given initial condition, the location of recompression $\bar{r}_3/r_b$, the corresponding inviscid condition $M_{3a}$, and the jet spread parameter $\sigma_{3a}$, must be known. The recompression point $\bar{r}_3/r_b$ is found from experimental data. The Mach number at 3, $M_{3a}$, is determined from the axisymmetric rotational method of characteristics solution. The jet spread parameter is determined from the equation given by Channapragada.[13]

## Discussion of Analytical and Experimental Results

A Fortran IV computer program combining the rotational method of characteristics and the base pressure solution technique was written for the University of Notre Dame UNIVAC 1107.

By using the overexpansion at the shroud exit the internal shock wave is detected in the vicinity of the exit corner. However, the question arises as to the effect of the overexpansion on the subsequent development and location of the shock. The value of the pressure to which the flow is expanded was determined by multiplying the percent overexpansion by the actual ambient pressure. The results show that changes in the amount of overexpansion have only a small effect on the shock wave location. The total deviation between the results for 75% and 95% overexpansion was less than 4%. This implies that an optimum value for the overexpansion can be selected without the need for extensive empirical correlations. Based on this and the experimental data, a value for the overexpansion of 85% was used for all analytical solutions presented.

#### Ambient Pressure

As air-breathing or rocket engines are operated at increasing altitudes, the ambient pressure decreases while the chamber pressure remains relatively constant. This variation of ambient pressure has a very pronounced effect on the flowfields of plug nozzle configurations. The comparison between theory and experiment are shown in Fig. 7 for the location of

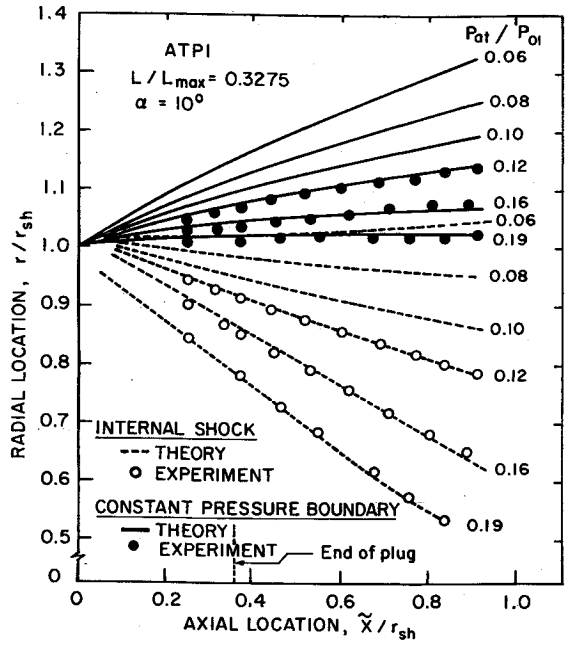


**Fig. 7 Effect of ambient pressure ratio on external jet boundary and internal shock wave locations.**

the internal shock wave and the constant pressure boundary for ATP1 and $L/L_{max} = 0.3275$. The results presented for this plug length are typical of the plug lengths studied. Solutions were obtained for several over-all pressure ratios for each of the plug lengths studied, in order to demonstrate the versatility of the analytical method. The over-all pressure ratios were chosen to give as large a variation as possible within the limits of the NTF during the closed wake operation. The theoretical solution detects the shock near the shroud exit, $\tilde{X}/r_{sh} \simeq 0.080$. However, because of the difficulty in obtaining data from the shadowgraphs this close to the exit, the plots for both the shock wave location and constant pressure boundary location are initiated at a dimensionless distance of $\tilde{X}/r_{sh} \simeq 0.2$ from the nozzle exit. Since the solution terminates at the trailing wake radius ratio, the results extend further downstream as the plug length is increased.

The correlation between experiment and theory for the constant pressure boundary location is excellent. The maximum discrepancy, equal to 5.4%, which is on the order of the experimental accuracy, occurred for the longest plug. As was the case with the internal shock, the agreement improves with distance downstream. Despite the large effects of the changing ambient pressure on the constant pressure boundary and internal shock wave shown in Fig. 7, the base pressure remains constant. This results from the fact that the wake is closed and that there is no interference in the near wake from the external flow.

### Nozzle Geometry

The analytical values of the base pressure ratio for the plug lengths studied for both ATP1 and ATP2 are compared with the experimental data in Fig. 4. Theoretical base pressures were not obtained for plug lengths smaller than $L/L_{max} \simeq 0.220$ for ATP1 and $L/L_{max} \simeq 0.135$ for ATP2. The reason for this is that shorter plugs would end upstream of the shroud exit plane. Reasonable agreement was obtained between experiment and theory for all but the shortest plug length for ATP1 as shown in Fig. 4. The difference between analytical and experimental base pressure was greater for this plug than for other plugs. The shadowgraphs for this plug indicated nothing unusual which might account for the lower base pressure. It is possible that the boundary layer on this shortest plug was not fully turbulent before separation at the plug corner. The base pressure depends on the degree of mixing in the viscous free shear layer and if this layer was transitional, the base pressure could be lower than if this layer is fully turbulent. In actual nozzle configurations, the area ratios will be greater and the nozzles will be larger, so the flow would always be expected to be fully turbulent in the boundary layer along the plug. The theory also correctly predicted the trend of decreasing base pressure with increasing area ratio. The agreement between theory and experiment improved for the increase in area ratio from ATP1 to ATP2. This was probably a consequence of the larger size of ATP2. With increased size, the viscous effects of the boundary layers became less influential. These viscous effects were not included in the calculations.

In the region of practical interest, the theoretical base pressure averages about 15% higher than the experimental values. While this agreement is not excellent, it does represent a substantial improvement over the solution which does not include the internal shock wave (i.e., Refs. 3 and 10). For ATP1 with $L/L_{max}$ equal to 0.4802, the experimentally determined value of the base pressure ratio is 0.070. Using the no-internal-shock solutions,[3] the analytical value of $P_b/P_{01}$ was 0.0879 as contrasted to a value of 0.0783 for the present method, which includes the internal shock. Thus, the error in the base pressure has been reduced from 27% to to 12%, or less than half the error for the no-shock solution. These results clearly demonstrate the necessity of including the internal shock for an accurate base pressure solution. With the internal shock included in the flowfield solution, the theoretical base pressure is still high. There are several possible reasons for this difference. The most plausible cause, however, is the viscous effects of the boundary layers on the nozzle surfaces. The nozzles used in this investigation had very small throat areas and therefore the viscous effects, which are not included, could be quite important. This effect would probably be less critical for larger nozzle configurations. Indeed the theoretical base pressure averages only 10% higher for the larger nozzle ATP2.

For truncated plug nozzles there are a large number of geometries possible. Having restricted this present study to the conical-plug cylindrical-shroud T-P nozzle, the effects of shroud length for ATP2 and plug angle for ATP1 on the flowfield and base pressure were documented analytically for closed wake operation. The corresponding effect of shroud length on the base pressure ratio is presented in Fig. 8. These calculations indicate that for 100% increase in shroud length, the base pressure ratio increases by about 104%. The longer the shroud, the greater is the internal expansion. The length of the shroud therefore, is determined by the amount of internal expansion desired.

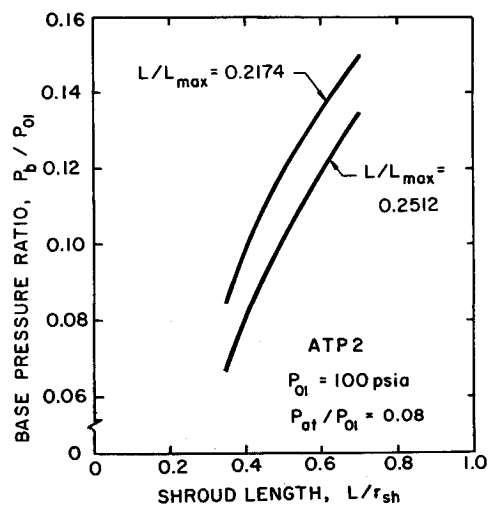


**Fig. 8 Effect of shroud length on base pressure ratio.**

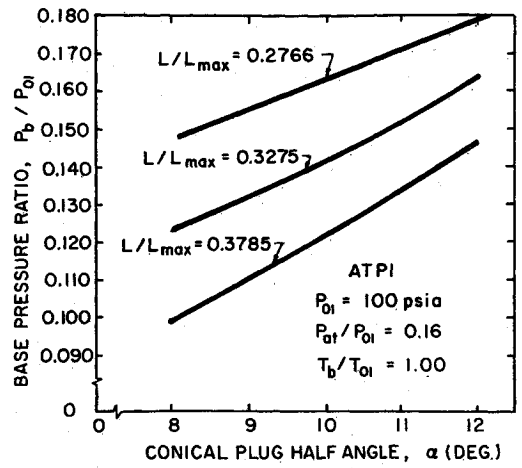


**Fig. 9 Effect of plug half-angle on base pressure ratio.**

The influence of plug angle on the constant pressure boundary and internal shock locations was studied. As the plug half-angle $\alpha$ increases, the expansion ratio from the throat to the shroud exit increases, although the throat area and over-all nozzle exit area remain constant. Thus, the Mach number at the shroud exit is higher and the static pressure is lower. The pressure at the shroud exit is still higher than the ambient but less expansion is necessary to meet the ambient pressure than for a smaller value of $\alpha$. Therefore, the constant pressure boundary moves toward the nozzle axis as $\alpha$ increases. The internal shock also moves toward the nozzle axis since the smaller expansion from the shroud exit pressure to the ambient pressure produces a smaller local overexpansion, in the vicinity of the shroud exit, which generates the internal shock. The effect of plug angle on base pressure ratio for three plug lengths is shown in Fig. 9. Plug length strongly influences the flow in the vicinity of the near wake and therefore the base pressure. The increase in base pressure ratio with increasing plug angle shown in Fig. 9 is consistent with the earlier analytical results of Mueller[7] which agreed very well with experiments.

## Conclusions

The experimental base pressure characteristics of truncated plug nozzles provide a convenient means of classifying the nozzle flow as having either an open or closed wake. It was found for constant ambient pressure that as upstream stagnation pressure increased, the base pressure of the open wake remained almost constant and in most of the open wake region it was equal to the ambient pressure. In general, this trend continued until the wake closed. An exception to this general trend occurred in a small region where the shock wave originating at the shroud exit impinged on the plug close enough to the base to produce a decrease and then an increase in the base pressure as the ambient pressure ratio decreased.

The analytical solution presented was found to accurately predict closed wake truncated plug nozzle flowfields (including the base pressure) over the range of nozzle configurations and over-all pressure ratios studied. The Hartree Technique used with the method of characteristics appeared to give very good results for the calculation of the inviscid part of the nozzle flowfield. This conclusion was verified by experimental data. The introduction of the overexpansion process at the shroud exit enabled the solution to detect the internal shock wave in the region where it develops in the actual flow. The shock wave location was accurately determined for all cases investigated.

The base pressure solution developed by Zumwalt and later modified by Mueller produced good agreement with experiment, and correctly predicted the variation in base pressure with plug truncation and area ratio. For the cases studied, $L/L_{max} \simeq 0.50$ represented the upper limit for the validity of the base pressure solution. The base pressure results were greatly improved by the inclusion of the internal shock wave in the over-all solution. The error in the base pressure was less than half of that obtained with the no-shock solution. It was further demonstrated that, in order to achieve this improvement, it is essential to have the internal shock originate near the shroud exit. If the overexpansion technique introduced (or a similar technique) is not used, the shock will originate downstream of the plug base where it cannot influence the base pressure. Analytical results showing the effects of shroud length and plug half-angle are also presented.

## References

[1] Sule, W. P., "A Study of Axisymmetric Truncated Plug Nozzle Flowfields Including the Influence of an Internal Shock Wave on the Base Pressure," Ph. D. dissertation, Jan. 1972, Dept. of Aerospace and Mechanical Engineering, Univ. of Notre Dame, Notre Dame, Ind.

[2] Hama, F. R., "Experimental Investigations of Wedge Base Pressure and Lip Shock," TR 32-1033, Dec. 1966, Jet Propulsion Lab., California Inst. of Technology, Pasadena, Calif.

[3] Hall, C. R., Jr. and Mueller, T. J., "Exploratory Analysis of Nonuniform Plug Nozzle Flowfields," *Journal of Spacecraft and Rockets*, Vol. 9, No. 5, May 1972, pp. 373–342.

[4] Weiss, R. F. and Weinbaum, S., "Hypersonic Boundary Layer Separation and the Base Flow Problem," Research Rept. 221, July 1965, Avco-Everett Research Labs., Everett, Mass.

[5] Zumwalt, G. W., "Analytical and Experimental Study of the Axially-Symmetric Supersonic Base Pressure Problem," Ph. D. dissertation, 1959, Dept. of Mechanical Engineering, Univ. of Illinois, Urbana, Ill.; also MIC 59–4589, University Microfilms Inc., Ann Arbor, Mich.

[6] Mueller, T. J., "Determination of the Turbulent Base Pressure in Supersonic Axisymmetric Flow," *Journal of Spacecraft and Rockets*, Vol. 5, No. 1, Jan. 1968, pp. 101–107.

[7] Mueller, T. J. and Hall, C. R., Jr., "Analytical Prediction of the Turbulent Base Pressure in Supersonic Axisymmetric Flow Including the Effect of Initial Flow Direction," AFFDL-TR-68-132, Sept. 1968, Air Force Flight Dynamics Lab., Air Force Systems Command, Wright-Patterson Air Force Base, Ohio.

[8] Hartree, D. R., *Numerical Analysis*, 2nd ed., Oxford University Press, London, 1958, Chap. X, pp. 257–263.

[9] Boynton, F. P., "Exhaust Plumes from Nozzles with Wall Boundary Layers," *Journal of Spacecraft and Rockets*, Vol. 5, No. 10, Oct. 1968, pp. 1143–1147.

[10] Mueller, T. J., Sule, W. P., and Hall, C. R., Jr., "Characteristics of Separated Flow Regions within Altitude Compensating Nozzles," UNDAS TN-129-PR-9, Jan. 1971, Univ. of Notre Dame, Notre Dame, Ind.

[11] Zumwalt, G. W. and Tang, H. H., "Transient Base Pressure Study of an Axisymmetric Missile Flying Head-On Through a Blast Wave," Research Rept. SBW-6, Feb. 1964, School of Mechanical Engineering, Oklahoma State Univ., Stillwater, Okla.

[12] Korst, H. H., Page, R. H., and Childs, M. E., "A Theory for Base Pressures in Transonic and Supersonic Flow," ME TN 392-2, May 1962, Univ. of Illinois, Urbana, Ill.

[13] Channapragada, R. S., "Compressible Jet Spread Parameter for Mixing Zone Analyses," *AIAA Journal*, Vol. 1, No. 9, Sept. 1963, pp. 2188–2190.